*Proc. Natl. Acad. Sci. USA*
Vol. 86, pp. 845–848, February 1989
Biochemistry

# Structural transitions in crystals of native aspartate carbamoyltransferase

(x-ray crystallography/protein dynamics/regulatory enzymes)

J. ERIC GOUAUX AND WILLIAM N. LIPSCOMB

Gibbs Chemical Laboratory, Harvard University, Cambridge, MA 02138

*Contributed by William N. Lipscomb, November 3, 1988*

ABSTRACT **Screened precession x-ray photographs of crystals of native aspartate carbamoyltransferase (EC 2.1.3.2, from *Escherichia coli*) ligated with L-aspartate and phosphate reveal the presence of a crystal unit-cell dimension that is intermediate between the T (tense) and R (relaxed) states. Characterizing the intermediate (I) crystal is a *c*-axis unit-cell dimension of 149 Å, halfway between the *c*-axis length of the T ($c$ = 142 Å) and R ($c$ = 156 Å) states, in the space group *P*321. Preservation of the *P*321 space group indicates that the intermediate crystal form retains a threefold axis of symmetry, and therefore the enzyme has at minimum a threefold axis; however, we do not know whether the molecular twofold axis is conserved. The I crystals are formed by soaking T-state crystals with L-aspartate and phosphate. By raising the concentration of L-aspartate we can further transform the I crystals, without fragmentation, to a form that has the same unit-cell dimensions as R-state crystals grown in the presence of *N*-(phosphonoacetyl)-L-aspartate.**

Aspartate carbamoyltransferase (EC 2.1.3.2) from *Escherichia coli* initiates the synthesis of pyrimidines by catalyzing the reaction between L-aspartate and carbamoyl phosphate to yield *N*-carbamoyl-L-aspartate and phosphate (ref. 1; see ref. 2 for a recent review). Poised at the beginning of the pathway, this cooperative enzyme helps control the flux of metabolites that eventually form the pyrimidine building blocks of DNA. The substrates L-aspartate and carbamoyl phosphate effect the homotropic cooperativity (3, 4). An end product of the pyrimidine pathway, cytidine 5′-triphosphate (CTP), can act as an allosteric inhibitor, while a product of the purine pathway, adenosine 5′-triphosphate (ATP), can function as an activator. CTP and ATP alter the enzyme's catalytic activity by decreasing and increasing its affinity for L-aspartate, respectively (1, 3). Structurally, the enzyme is a dodecameric complex of two catalytic subunits ($2c_3$) and three regulatory subunits ($3r_2$) as shown in Fig. 1 (5, 6). The isolated catalytic subunits turn over L-aspartate and carbamoyl phosphate while possessing no cooperative properties and the regulatory subunits bind the allosteric effectors CTP and ATP without exhibiting any catalytic properties (3, 4, 7).

The Monod–Wyman–Changeux (MWC) model of allosteric transitions (8) has provided a valuable framework for understanding the homotropic cooperative properties of *E. coli* aspartate carbamoyltransferase. However, two fundamental tenets of the MWC model have never been confirmed. The first concerns the number of reversibly accessible quaternary conformational states, and the second pertains to the conservation of molecular symmetry throughout the allosteric transition. Although the MWC model asserts that there can be more than two quaternary conformational states, it is generally assumed that there are only two stable quaternary states. To address these questions and the more detailed problems concerning the propagation of indirect interactions between the catalytic and regulatory binding sites, we performed a series of crystallographic experiments in which crystals of aspartate carbamoyltransferase were cocrystallized and/or soaked with combinations of substrates, products, and their analogues. Here we report the results of experiments in which T-state crystals were soaked in solutions containing the substrate L-aspartate and one of the products, inorganic phosphate.

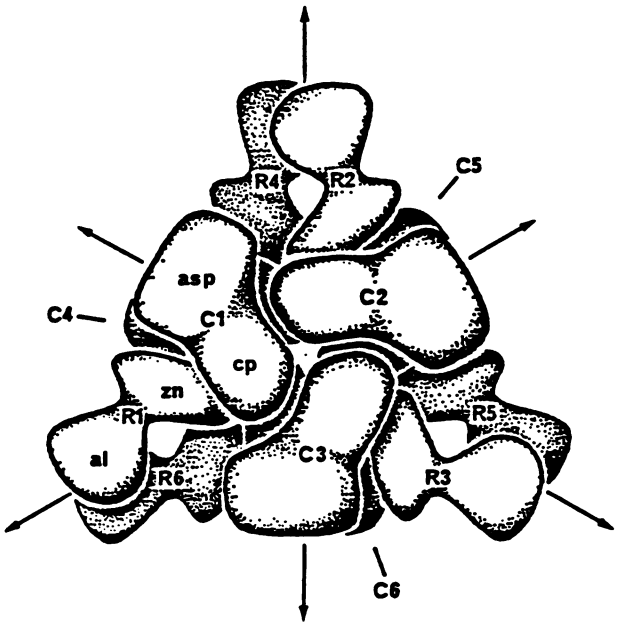


FIG. 1. Domain and subunit structure of aspartate carbamoyltransferase. The threefold axis is perpendicular to the plane of the page, while the twofold axes lie in the plane of the page. The polypeptide chains *c*1, *c*2, *c*3, *r*1, *r*2, and *r*3 comprise the upper half of the holoenzyme; the lower half is composed of the chains *c*4, *c*5, *c*6, *r*4, *r*5, and *r*6. Also labeled are the aspartate (asp), carbamoyl phosphate (cp), zinc (zn), and allosteric (al) domains.

The homotropic cooperativity observed for the holoenzyme ($c_6r_6$) is typically rationalized in terms of a concerted transition between two quaternary conformations, the T (tense) and R (relaxed) states (9–13). As defined by the CTP-ligated T-state and the *N*-(phosphonoacetyl)-L-aspartate (PALA)-ligated R-state structures, the quaternary structural changes involved in the T → R transition can be

The publication costs of this article were defrayed in part by page charge payment. This article must therefore be hereby marked "*advertisement*" in accordance with 18 U.S.C. §1734 solely to indicate this fact.

Abbreviations: T state, quaternary conformation of aspartate carbamoyltransferase characterized by a *c*-axis unit-cell dimension of 142 Å in the space group *P*321; R state, quaternary conformation that has a *c*-axis length of 156 Å in the same space group; I crystal, crystal form that is halfway between the T and R states as defined by the length of the *c* axis in the *P*321 space group; MWC, Monod–Wyman–Changeux; PALA, *N*-(phosphonoacetyl)-L-aspartate.

described as follows. The separation between the catalytic trimers increases by 12 Å along the threefold axis and they rotate relative to each other by 5°, also around the threefold axis (total rotation, 10°), while the three regulatory dimers rotate by 15° about the three molecular twofold axes. Although the two-state model is consistent with many experiments, other data indicate that there are more than these two conformational states available to the enzyme (14, 15). An important element of any study probing the nature of the allosteric transition concerns the specific substrates or substrate analogues used in the experiments. For example, we recently determined the structure of the ternary complex of carbamoyl phosphate, succinate, and aspartate carbamoyltransferase (16). One of the conclusions from this experiment is that carbamoyl phosphate and succinate seem to be excellent analogues of PALA. It remains to be seen how the structure of a PALA–enzyme (17) or a carbamoyl phosphate–succinate–enzyme (16) complex is related to a true carbamoyl phosphate–aspartate–enzyme or a reaction intermediate–enzyme complex.

In this study, we choose to focus on the interactions of L-aspartate and phosphate with crystals of aspartate carbamoyltransferase for a number of reasons. (*i*) In the presence of phosphate, L-aspartate binds tightly to the enzyme (18). (*ii*) When bound to the catalytic subunit, the combination of phosphate and L-aspartate gives a UV difference spectrum that is intermediate between the difference spectrum observed for phosphate and the difference spectrum of carbamoyl phosphate and succinate (19). (*iii*) In phosphate buffer at low carbamoyl phosphate concentration, the Eadie plot (20) as a function of carbamoyl phosphate concentration is almost linear, indicating that the cooperativity of the holoenzyme is dramatically reduced (13). (*iv*) At a concentration of 15 mM L-aspartate in phosphate buffer, the sedimentation coefficient for the native enzyme decreases by 1.8%, compared to a decrease of 3.0% in the presence of saturating PALA (13). Taken individually, each of these experiments does not have a unique interpretation; none of the experiments can distinguish between an intermediate conformation of the holoenzyme (or the catalytic subunit) or a displacement in the T $\rightleftharpoons$ R equilibrium toward the R state. However, as we document here, phosphate and L-aspartate stabilize an intermediate crystal form of the enzyme in the *P*321 space group at pH 7. Furthermore, additional experiments have shown that the enzyme can readily undergo the T $\rightarrow$ R transition within a crystal of the *P*321 crystal form at pH 7 (unpublished results). Since the transitions in the crystal slowly take place under conditions of moderate substrate, product, or inhibitor concentrations, we speculate that the intermolecular contacts in the crystal impose predominately a kinetic, rather than a thermodynamic, barrier to the conformational changes.

## MATERIALS AND METHODS

Native aspartate carbamoyltransferase was isolated as described (21) from the EK1104 strain of *E. coli*, which contained the plasmid pEK2 carrying the entire native *pyrBI* operon, in the laboratory of E. R. Kantrowitz. Protein concentration was determined from $A_{280}$ by assuming an extinction coefficient of 0.59 $cm^2$/mg (22) for the holoenzyme. L-Aspartate, phosphate, citrate, CTP, 2-mercaptoethanol, ethylenediaminetetraacetic acid (EDTA), 4-morpholineethanesulfonic acid (Mes), and polyethylene glycol 8000 were purchased from Sigma.

The enzyme, stored at −20°C as a 25-mg/ml solution in 1:1 (vol/vol) glycerol/storage buffer (40 mM $K_2PO_4$/2 mM 2-mercaptoethanol/0.2 mM EDTA, pH 7.0), was dialyzed for 24 hr against storage buffer prior to crystallization. Subsequently, the enzyme solution was dialyzed for an additional 24 hr against 1 mM citrate/1 mM CTP/2 mM 2-mercaptoethanol/0.2 mM EDTA, with the pH adjusted to 7.0 with NaOH. The enzyme solution was then diluted to 20 mg/ml and filtered through a 0.22-μm filter (Millipore GV). Crystallization was effected by dialyzing the enzyme solution at room temperature against 40 mM sodium citrate/1 mM 2-mercaptoethanol/0.2 mM EDTA/1 mM CTP with the pH adjusted to 5.8 with HCl. Typically, hexagonal plates in the space group *P*321 ($a = b$ = 122.2 Å and $c$ = 142.2 Å) grew in 2–3 weeks. After the crystals reached a sufficient size, they were transferred to 20 mM Mes/2 mM 2-mercaptoethanol/0.2 mM EDTA/15% (wt/vol) polyethylene glycol 8000 at pH 7 for at least 24 hr to dilute the concentration of citrate. Then the crystals were placed in a large excess of standard soaking buffer (40 mM phosphate/2 mM 2-mercaptoethanol/0.2 mM EDTA/15% polyethylene glycol 8000) containing various concentrations of L-aspartate and with the pH always adjusted to 7 with NaOH. The most effective method for obtaining I crystals consisted of slowly increasing the concentration of L-aspartate in the standard soaking buffer to 40 mM over a period of days. Although some of the crystals subjected to these conditions developed cracks visible in a light microscope, most of the crystals were not damaged. The primary lattice of the I crystals obtained by this procedure belongs to the space group *P*321 with unit-cell dimensions $a = b$ = 122 Å and $c$ = 149 Å. The unit-cell dimensions of the weaker superlattice are, tentatively, $a = b$ = 122 Å and $c$ = 300 Å, but the space group has not yet been conclusively determined. By careful inspection of each soaking experiment and removal of the T-state crystals, once grown, from the dialysis chambers, we assured that there was no chance that during the soaking procedure, the T-state crystals dissolved and the I crystals grew from the dissolved protein.

The screened x-ray precession photographs were taken from crystals mounted in flame-sealed silanized glass capillaries with soaking buffer on either side of the crystals. An Elliot GX-6 rotating anode operating at 40 kV and 20 mA and equipped with a Ni filter produced the Cu $K_\alpha$ x-rays. Typically, an 8° screened precession photograph was recorded on CEA 25 film using a Supper oscillation/precession camera in ≈16 hr.

## RESULTS

I crystals of aspartate carbamoyltransferase, where the primary lattice belongs to the space group *P*321 and has unit cell dimensions of $a = b$ = 122 Å and $c$ = 149 Å, can be prepared by soaking T-state crystals (space group also *P*321, $a = b$ = 122 Å and $c$ = 142 Å) in solutions of phosphate and L-aspartate at pH 7. These crystals, slightly less well ordered than crystallized T- or R-state crystals, diffract to 3.0 Å. Shown in Fig. 2*B* is a screened precession x-ray photograph of the ($h$, 0, $l$) zone of an I crystal. In Fig. 2 *A* and *C* are screened precession photographs of the same zone (at about the same scale) of T- and R-state crystals, respectively. Not only does the $c$-axis unit-cell dimension of the I crystal differ from those of the T- and R-state crystals, but the intensities of reflections with the same Miller index are frequently different. Interestingly, we have discovered that 80 mM L-aspartate in the soaking buffer at pH 7 will transform T-state crystals to poorly ordered crystals that have the same unit-cell dimensions as crystallized R-state crystals. Another combination of ligands that induces the T $\rightarrow$ I transition in *P*321 crystals is L-malate and phosphate. However, we have found so far that the combination of phosphate and L-aspartate is the most effective in stabilizing the I crystals.

Close inspection of precession photographs of the ($h$, 0, $l$) zone of I crystals indicates the presence of a superlattice with a $c$-axis unit-cell dimension that is approximately twice the 149-Å axis, or 300 Å, giving rise to a supercell. Although we have not been able to conduct an exhaustive survey of the reciprocal space of the superlattice due to the weakness of the reflections, at this point it appears that the $a$ and $b$ unit-cell

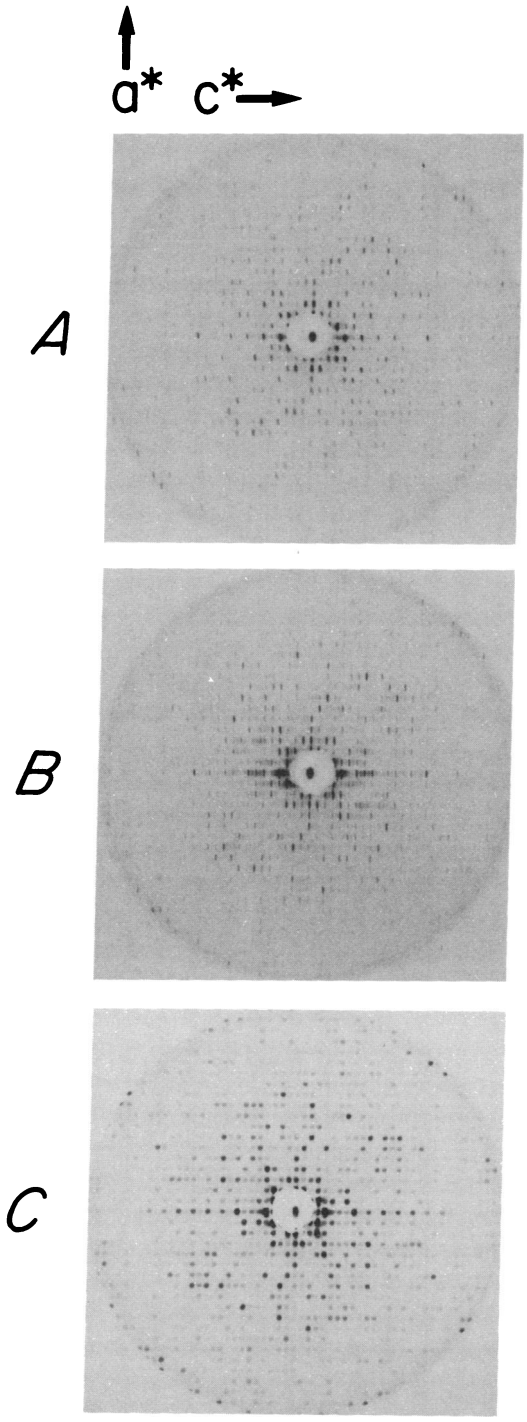


FIG. 2. Screened precession photographs of the ($h$, 0, $l$) zone of T-state ($A$), I ($B$), and R-state ($C$) crystals. The $c^*$ axis is horizontal, and the $a^*$ axis is vertical. In these full-size photographs, the crystal-to-film distance used in the experiments was identical. Consequently, a direct, albeit approximate, measurement of the $c$ unit-cell dimensions can be made by measuring the distance between reflections on the $c$ axis in millimeters, taking the inverse of that number, and multiplying the result by 154.2 Å·mm. In $B$ on the (0, 0, $l$) zone, there are a number of clearly visible superlattice reflections occurring between the brighter and more sharp primary lattice reflections. If we index the photograph by using the superlattice, two of these reflections have indices (0, 0, 13) and (0, 0, 15), for example.

dimensions of the supercell are the same as those for the smaller, primary unit cell, which has a $c$-axis unit-cell dimension of 149 Å. Of course, a doubling of the unit cell along the $c$ axis implies that the number of molecules in the unit cell increases from two to four. Unfortunately, the space group of the supercell has not been conclusively determined, because cone axis, precession, and oscillation photographs of the zero and upper levels of the ($h$, $k$, 0) zone show only weak superlattice reflections. The use of synchrotron radiation might help resolve this problem. Experiments in which the crystal temperature was lowered from 20°C to −5°C for up to 24 hr were not successful in abolishing, or even noticably reducing, the presence of the superlattice.

## DISCUSSION

Although many models have been proposed to explain cooperative properties in proteins, the MWC model, when applied to the homotropic cooperativity of aspartate carbamoyltransferase, has been the most successful in accommodating many different sources of experimental data. However, two of the six statements upon which the MWC model is based have proven difficult to confirm. The first concerns the number of states that are reversibly accessible to the protein, and the second declares that the molecular symmetry of the protein is conserved in going from one state to another (8).

The symmetry constraint has been established down to the secondary structural level by x-ray crystallography for the T and R states, but there is no information concerning the symmetry of intermediate states. The space group in which the T- and R-state structures have been solved and thoroughly refined is $P321$. Here, there are two molecules in the unit cell with one-third of a molecule in the asymmetric unit. The asymmetric unit is the smallest unique motif from which the unit cell and the entire crystal can be constructed. Contained in the asymmetric unit is the $c_1r_1r_4c_4$ entity, where one $cr$ unit resides in the upper half of the holoenzyme and the other $cr$ unit belongs in the lower half (Fig. 1). In the $P321$ space group, the molecular threefold axis of the holoenzyme corresponds to the crystallographic threefold axis. The crystallographic threefold operation generates the holoenzyme ($c_6r_6$) from the $c_2r_2$ moiety in the asymmetric unit; the crystallographic twofold operation then produces the second molecule in the unit cell. Consequently, if an intermediate structure produced from $P321$ T-state crystals still belongs to the $P321$ space group, the threefold symmetry axis would be conserved. Screened precession x-ray photographs of the ($h$, 0, $l$), ($h$, $h$, $l$), ($h$ + 1, $h$, $l$), ($h$, $k$, 0), and ($h$, $k$, 1) zones of I crystals show that the space group is $P321$ for the primary lattice with the $c$-axis cell length of 149 Å. However, there is no crystallographic analogue of the molecular twofold axis. Hence, the molecular twofold axis is not constrained by the symmetry of the space group. In the R-state structure determined in the presence of the bisubstrate analogue PALA, there are no significant deviations in the main-chain atoms from the molecular twofold symmetry (23). Yet in the T-state structure, where the allosteric ligand CTP is bound to the regulatory chain, there are two regions of the molecule that violate the molecular twofold symmetry (24). Unfortunately, the basis for the symmetry violations is not apparent; either the crystal lattice environment or the inherent asymmetry of the enzyme could be responsible. Based on the space group of the I crystals, we know that the threefold axis is preserved; conclusions regarding the presence of a molecular twofold axis cannot be made until the structure has been solved.

The symmetry of the supercell with a $c$ unit-cell dimension of about 300 Å has not yet been determined because of the weakness of the reflections defining the superlattice. The periodic disorder seen in the precession photos of the I crystals is reminiscent of the "ghost" reflections observed on x-ray photographs of the dahlemense strain of tobacco mosaic virus (25). In that study, the additional reflections appearing on half-order layer lines were interpreted as arising

from "... a regular perturbation of the arrangement of the outer part of the protein subunit" (25). At this point, we do not have such a specific understanding of the structural elements responsible for the superlattice reflections. However, there are two extreme possibilities in which the packing of the molecules could give rise to the 300-Å repeat. One such possibility is that there are regularly repeating layers of T- and R-state molecules and that the ligands do not stabilize an intermediate conformation of the enzyme, but rather they simply displace the T $\rightleftharpoons$ R equilibrium toward the R state. In contrast, the superlattice reflections might arise from some regular periodic perturbation in the packing, or conformation, of molecules whose quaternary conformation is intermediate between the T and R states. Interestingly, the reflections defining the superlattice have a more diffuse appearance when compared to the primary lattice reflections. When the terms recommended by Caspar *et al.* (26) are used, the variational component of the scattering from the crystal, defined as the scattering arising from structural variations of the molecule, appears to be greater for the superlattice reflections than for the primary lattice reflections.

In the crystal, we have determined that there are at least three distinct *c*-axis unit-cell dimensions for the native holoenzyme, the T, I, and R states. We have also shown that phosphate and L-aspartate can transform T-state crystals to I crystals and, by further raising the concentration of L-aspartate, to a crystal form with the same unit-cell dimensions as PALA-ligated R-state crystals. In addition, the kinetic experiments of Howlett *et al.* (13), done in phosphate buffer at subsaturating carbamoyl phosphate and saturating L-aspartate concentrations, showed that the holoenzyme has lost almost all cooperativity and has an R-state-like activity. These data provide evidence that the conformation that is stabilized by phosphate and L-aspartate is a cooperatively competent species on the T $\rightarrow$ R isomerization pathway. Further, we propose that the gross conformation be tested by low-angle x-ray scattering in solution, because of our belief that the transformation that we find within a crystal suggests, but does not prove, that the intermediate conformation is molecular in origin and not due to crystal constraints.

Inspection of the PALA–enzyme or carbamoyl phosphate–succinate–enzyme complexes indicates that these R-state structures might be more nearly similar to an enzyme–reaction intermediate complex than to an enzyme–substrate complex. In other words, the PALA- and carbamoyl phosphate/succinate-ligated enzymes might represent the structure of the enzyme after the bond between L-aspartate and carbamoyl phosphate has formed. We conjecture that the I crystal form is composed primarily of enzyme molecules that are in a quaternary conformation that is intermediate between the T and R states; we will call this the I state to differentiate it from the I crystal form. This state might be a quaternary conformation induced upon substrate binding, possibly before the chemical reaction has taken place. The isomerization of the I state to the R state might then occur during the reaction between the substrates. It is also possible that the I state of the enzyme is reached during product release. Of course, since there are six active sites on the holoenzyme, it is difficult to determine how the quaternary structure will be affected by different processes occurring in each of the active sites. Some progress toward the understanding of this problem has been made by studies of the reverse reaction in the presence of subsaturating concentrations of PALA (27). Unfortunately, it is not clear how the results from these experiments could be used to interpret the mechanism of the enzyme in the presence of L-aspartate and carbamoyl phosphate. We also speculate that once the enzyme has isomerized from the T to the I state, many of the subunit contacts that are responsible for endowing the enzyme with its cooperative properties are lost. Once aspartate carbamoyltransferase has reached the I state, it might functionally appear as an R-state enzyme with a high affinity for L-aspartate, high activity, and greatly diminished cooperativity. We remind the reader that the speculations contained in this paragraph should be taken as such and that any definitive conclusions will have to await the solution of the structure.

It might be possible to stabilize the putative I state of aspartate carbamoyltransferase by making single and double amino acid mutants. For example, one idea for a double amino acid mutant is to make one mutation that destabilizes the $c_1c_4$ interface in the T state and another amino acid change that disfavors the formation of the carbamoyl phosphate domain–aspartate domain interface in the R state. In addition, stabilization of the I state might be promoted by organic solvents, different pH conditions, and other substrate or product analogues, to mention a few of many possibilities.

M. F. Perutz, F. A. Quiocho, and D. C. Rees are acknowledged for providing helpful comments on the manuscript. We thank E. R. Kantrowitz and his group for help in the preparation of large quantities of enzyme and the National Institutes of Health for support (Grant GM06920).

1. Yates, R. A. & Pardee, A. B. (1956) *J. Biol. Chem.* **221,** 743–756.
2. Kantrowitz, E. R. & Lipscomb, W. N. (1988) *Science* **241,** 669–674.
3. Gerhart, J. C. & Pardee, A. B. (1962) *J. Biol. Chem.* **237,** 891–896.
4. Bethell, M. R., Smith, K. E., White, J. S. & Jones, M. E. (1968) *Proc. Natl. Acad. Sci. USA* **60,** 1442–1449.
5. Weber, K. (1968) *Nature (London)* **218,** 1116–1119.
6. Wiley, D. C. & Lipscomb, W. N. (1968) *Nature (London)* **218,** 1119–1121.
7. Gerhart, J. C. & Schachman, H. K. (1965) *Biochemistry* **4,** 1054–1062.
8. Monod, J., Wyman, J. & Changeux, J.-P. (1965) *J. Mol. Biol.* **12,** 88–118.
9. Changeux, J.-P., Gerhart, J. C. & Schachman, H. K. (1968) *Biochemistry* **7,** 531–538.
10. Wu, C.-W. & Hammes, G. G. (1973) *Biochemistry* **12,** 1400–1408.
11. Howlett, G. J. & Schachman, H. K. (1977) *Biochemistry* **16,** 5077–5083.
12. Blackburn, M. N. & Schachman, H. K. (1977) *Biochemistry* **16,** 5084–5091.
13. Howlett, G. J., Blackburn, M. N., Compton, J. G. & Schachman, H. K. (1977) *Biochemistry* **16,** 5091–5099.
14. McClintock, D. K. & Markus, G. (1968) *J. Biol. Chem.* **243,** 2855–2862.
15. McClintock, D. K. & Markus, G. (1969) *J. Biol. Chem.* **244,** 36–42.
16. Gouaux, J. E. & Lipscomb, W. N. (1988) *Proc. Natl. Acad. Sci. USA* **85,** 4205–4208.
17. Krause, K.L., Volz, K. W. & Lipscomb, W. N. (1987) *J. Mol. Biol.* **193,** 527–553.
18. Porter, R. W., Modebe, M. O. & Stark, G. R. (1969) *J. Biol. Chem.* **244,** 1846–1859.
19. Collins, K. D. & Stark, G. R. (1971) *J. Biol. Chem.* **246,** 6599–6605.
20. Eadie, G. S. (1942) *J. Biol. Chem.* **146,** 85–93.
21. Nowlan, S. F. & Kantrowitz, E. R. (1985) *J. Biol. Chem.* **260,** 14712–14716.
22. Gerhart, J. C. & Holoubek, H. (1967) *J. Biol. Chem.* **242,** 2886–2892.
23. Ke, H.-M., Lipscomb, W. N., Cho, Y. J. & Honzatko, R. B. *J. Mol. Biol.*, in press.
24. Kim, H. K., Pan, Z., Honzatko, R. B., Ke, H.-M. & Lipscomb, W. N. (1987) *J. Mol. Biol.* **196,** 853–875.
25. Caspar, D. L. D. & Holmes, K. C. (1969) *J. Mol. Biol.* **46,** 99–133.
26. Caspar, D. L. D., Clarage, J., Salunke, D. M. & Clarage, M. (1988) *Nature (London)* **332,** 659–662.
27. Foote, J. & Schachman, H. K. (1985) *J. Mol. Biol.* **186,** 175–184.